



NUMERICAL EVALUATION OF THE TEMPORAL VARIATION OF VIBRATIONS INDUCED BY UNDERGROUND TRAINS

Marco Acquati¹ Nicola Pontani^{2*} Luca Martinelli² Cristina Jommi^{2,3}

¹MM S.p.A., via del Vecchio Politecnico 8, Milano, Italy

²Department of Civil and Environmental Engineering, Politecnico di Milano, Italy

³Faculty of Civil Engineering and Geosciences, TU Delft, The Netherlands

ABSTRACT

The change in the dynamic response of shallow soils as caught by two geophysical test campaigns is exploited to numerically predict the variation in the ground borne vibrations induced by the passage of underground trains. Multiple causes may lead to a variation in the perception of vibrations over time: from an increase in the train load to the roughness of the railway track, from the increase of the train speed to the modification of the dynamic response of the surrounding soil. In the present study, special attention is devoted to the effect of the hydrological regime on the latter. Two scenarios were calibrated on the results of repeated geodynamic tests on the same site in Milano but at two different times. The two investigations revealed differences in the dynamic response of above-ground soils which can be related to different saturation profiles. The passage of a typical convoy is simulated in the time domain. Differences between the two scenarios are highlighted together with the role played by the static axle load of the train. Furthermore, comparisons with recorded accelerations are provided to validate the model.

Keywords: *ground borne vibrations, geophysical investigation, underground trains, FE method*

1. INTRODUCTION

The role played by a change in the dynamic response of the soil - tunnel system on the ground borne vibrations produced by underground trains has seldom been investigated [1]. Nevertheless, small attention has been paid in the past on the interference of the water regime within the soil on the response of the infrastructure. As a matter of fact, the position of the water table [2-3], together with the conditions of partial saturation affecting the shallowest layers of soil [4] may produce variations in the vibrations induced by the passage of trains. This situation is particularly crucial for the tunnels of the M1 metro line in Milano, Italy. To quantify possible changes in the dynamic behaviour of the soil along the Milano M1 metro line, the results of two geophysical tests conducted by Metropolitana Milanese (MM) at the same site, but in two different moments in time, have been exploited. Differences between the two tests are interpreted as the consequence of different profiles of degree of saturation in the two circumstances.

To numerically study the effects induced by the change in the soil conditions on the environmental vibration due to metro train passage, the profiles of the physical and mechanical quantities that arose from the two investigations are implemented in a 2D finite element model, along with a representative geometry for the M1 tunnel. This reference M1-like tunnel is then subjected to a load time-history, reproducing the passage of a train. The frequency content of the load is generated by the load spectrum reported in the standard [5] devoting particular attention to the role played by the static weight of the train. Hydro-mechanical dynamic drained analyses have been performed by means of the finite element code Tochnog.

*Corresponding author: nicola.pontani@polimi.it

Copyright: ©2023 Marco Acquati et al. This is an open-access article distributed under the terms of the Creative Commons Attribution 3.0 Unported License, which permits unrestricted use, distribution, and reproduction in any medium, provided the original author and source are credited.

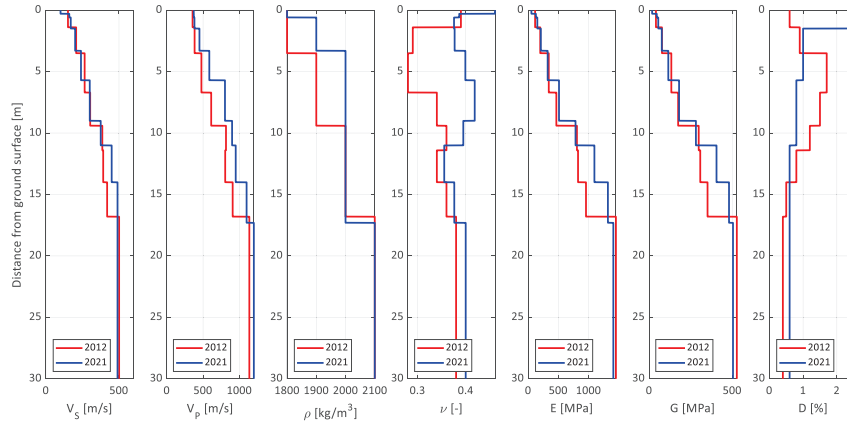


Figure 1 Results from geophysical tests.

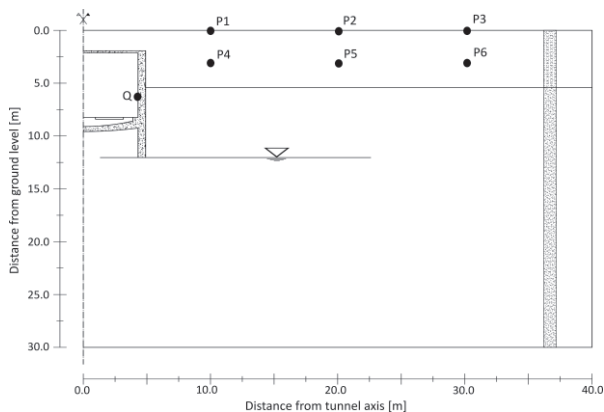


Figure 2 Reference 2D domain implemented in the FE model with a typical M1 metro-line tunnel in Milano.

2. MATERIALS AND METHODS

2.1 Site characteristics identification

The profile of shear and compression waves, V_{sv} and V_p , density, ρ , average dynamic values of the Poisson coefficient, ν , Young modulus, E , shear stiffness, G , and damping ratio, D , retrieved from the two geophysical campaigns conducted in March 2012 and April 2021, at the same site in Milano, are reported in Fig. 1. The techniques used in the geophysical investigations included: P-wave seismic tomography, M.A.S.W. (Multistation Analysis of Surface Waves), RE.MI. (Refraction Microtremor) and HVSr (or Nakamura Technique) prospectations. Available piezometric measurements between 2012 and 2021 identify

an average annual variation in the position of the water table, which maintains a depth of 12.0 - 14.0 m from the ground surface. The analysis of borings collected near the site suggests a stratigraphy mainly characterized by sands and gravel, with a shallowest remolded silty-sand layer, as typical for the Milano area. From the study of rainfall patterns in the two geophysical testing periods, the soil above the water table is expected to be wetter in April 2021 than in March 2012, as the total cumulative rainfall in the previous month, measured by a rain gauge close to the investigation site, amounts to 47.8 mm and 18.2 mm in year 2021 and 2012 respectively. Therefore, differences highlighted by geophysical results may be directly connected to this.

2.2 Numerical model

Two 2D finite element models were built in Tochnog to reproduce the tunnel configuration depicted in Fig. 2 with the material property distribution depicted in Fig. 1. For both situations, the water table is located at a depth of 12.1 m from the surface, i.e., at the base of the two walls, as data suggest small variations between 2012 and 2021. Materials are modelled as linear elastic media with Rayleigh viscous damping. The physical-mechanical properties of the tunnel and superstructure components were assigned from technical standards indications and previous studies. For the reinforced concrete, density, elastic modulus and Poisson's coefficient are set to 2.5 Mg/m^3 , $2.5 \cdot 10^4 \text{ MPa}$ and 0.2, respectively. For the ballast and wooden sleepers, the same quantities are 1.3 and 1.0 Mg/m^3 , $3.0 \cdot 10^2$ and $9.4 \cdot 10^2 \text{ MPa}$, 0.3 and 0.1, respectively. In the frequency range of interest for the dynamic response of the system (10 - 80 Hz), the damping-frequency curve of the reinforced concrete and ballast were calibrated to have damping ratios smaller than

5.0% and 3.0%, respectively. The passage of a train was modelled in the time domain as a vertical load time-history, directly applied to the sleeper, over the rail footprint. The load $q(t)$ is obtained as the superposition of a static component, q_s , and a dynamic one, $q_d(t)$:

$$q(t) = q_s + q_d(t) \quad (1)$$

The former is the result of the total weight of the train, which depends on the static load transmitted by each axle to the tracks, Q_s , the number of axes per bogie, bogies per coach and coaches, N_{AB} , N_{BC} and N_C . Following an approach similar to Xu et al. [6], the static pressure is computed as

$$q_s = Q_s N_{AB} N_{BC} N_C / 2BL \quad (2)$$

being $B = 0.15$ m the width of the rail at the contact with the sleeper and L the total length of the train. Details on the values assumed for these quantities are provided in Tab. 1. The static axle load for the case reported in [5] is $Q_{s160} = 160.0$ kN/axle. Since the train running along the M1 metro line in Milano are lighter, a second static load has been set to $Q_{s60} = 60$ kN/axle, to compare the effect of the different weight of the train.

Table 1 Number of axes per bogie, N_{AB} , bogies per coach, N_{BC} and coaches, N_C . L is the total length of the train considered in the simulations.

N_{AB}	-	2
N_{BC}	-	2
N_C	-	6
L	m	107.0

The dynamic component, is deduced from the load spectrum given in [5] and defined for the i -th twelfths of octave frequency band as:

$$\varepsilon(f_i) = Q_d(f_i) / Q_s \quad (3)$$

Assuming the process to be random and stationary [8], from the estimation of the power spectral density function associated to Eqn. (3) a possible temporal realization can be derived [9]. As the train is supposed to cross the section at a speed of 50.0 km/h, the signal is cut at a length of 7.7 s. Finally, two ramps of arbitrary length of 1.025 s are added to simulate the arrival and the removal of the train from the section, providing a non-stationary shape to the process.

The two loads enforced in the models are depicted in Fig. 3. They differ just for the static weight of the train, i.e., Q_{s160} and Q_{s60} .

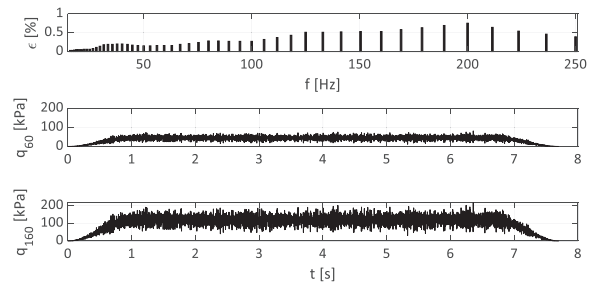


Figure 3 Non-dimensional dynamic load spectrum [5] and time-history of the applied loads.

The reference domain is discretized with 21245 4-node isoparametric finite elements with both displacement and pore pressure dofs activated for the soil. Their dimensions were suitably fixed considering the frequency range of interest of the induced signal in order to have a reliable representation even for the highest frequencies, i.e., up to 150 Hz. The FE discretization is characterized by a denser area around the tunnel where the elements have dimensions of 0.2 m. Outside, dimensions increase to an average size of 0.5 m, as the soil is proved to dampen out frequencies higher than 100 Hz at those distances. Elements are refined to 0.1 m at the right sleeper, where the vertical train load is enforced, to have a sufficient number of nodes over which to distribute the load. At the boundaries, viscous dampers were implemented to avoid spurious reflections of stress waves (Fig. 4). Damping coefficients are estimated from the elastic properties of the adjacent elements. Each simulation begins with a first step in which gravity is switched on to generate the correct static initial conditions. Then, the passage of the train is simulated considering the dynamic response of the system.

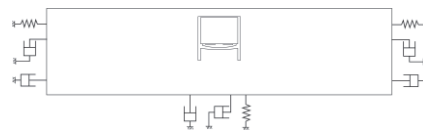


Figure 4 Boundary conditions implemented.

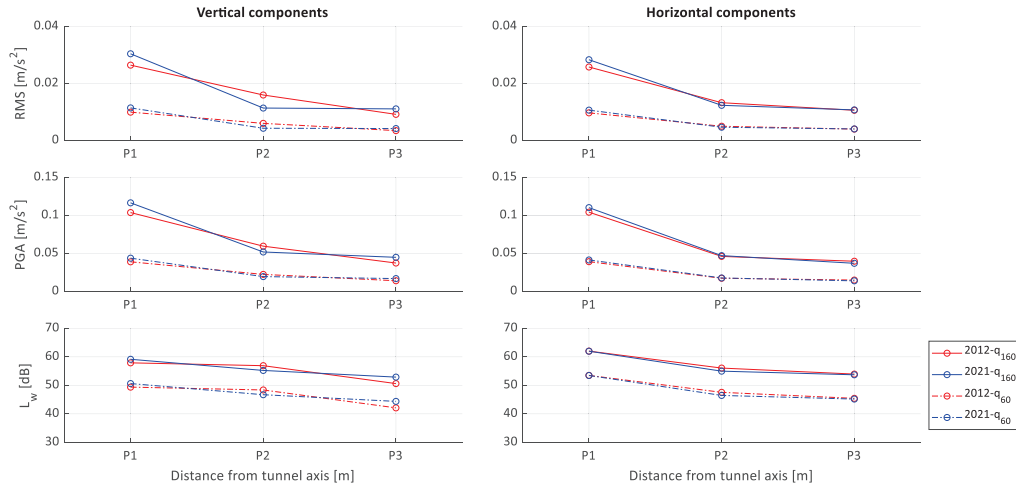


Figure 4 Root Mean Square, Peak Ground Acceleration and weighted acceleration level [6] for control points at ground surface (see Fig. 1).

3. RESULTS

The ground motion, induced by the train load depicted in Fig. 3 may be concisely evaluated by means of few indicator quantities [10] such as the Root Mean Square, *RMS*, and the Peak Ground Acceleration, *PGA*, which provide a picture of the average oscillation of the signal and maximum value in the considered period of interest, respectively. Nonetheless, the role played by human perception in the quantification of vibration exposure should be considered. For the sake of simplicity, the approach suggested by [5] can be used to this end, providing the estimation of the acceleration-weighted levels, *L_w* taking care of two main aspects: (i) the effects of vibrations of different frequency are cumulative and (ii) vibrations are perceived differently depending on the frequency. This definition holds then [5]:

$$L_w = 10 \text{Log} \sum 10^{L_{w,i}/10} \quad (4)$$

The levels *L_{w,i}* are derived from the thirds of octaves Fourier amplitude acceleration spectra, *a_i*, as

$$L_i = 20 \text{Log}(a_i/a_0) \quad (5)$$

then weighted with the frequency filter referred to vibrations propagating through the human body back [5]. The reference acceleration *a₀* is 10⁻⁶ m/s². A spatial view of the previous quantities is provided in Fig. 4 for control points P1, P2 and P3, located on the ground surface to the

right-hand side of the tunnel, for the static train loads, *Q_{s160}* and *Q_{s60}*. In both situations, accelerations decrease with increasing distances from the tunnel axis, as a result of geometric attenuation and material damping. The static weight of the train produces effects at almost every distance. The main differences are clearly induced in the neighborhood of the tunnel, where *RMS*, *PGA* and *L_w* undergoes an increase of 200%, 170% and 17% passing from *Q_{s60}* to *Q_{s160}* for the vertical acceleration. A similar behaviour can be highlighted for the horizontal component. A different response of the system is also expected when different dynamic configurations are present, i.e., 2012 and 2021 cases. The variations are mainly emphasized with the greater static load with differences of about 1-2 dB at almost every distance from the axis of the tunnel. A spatial view of the motion induced by the train in the volume of soil around the tunnel is provided in Fig. 5 where the acceleration spectral ratios are reported for two control points on the ground, i.e., P1 and P2, and at a depth of -3.0 m from them, i.e., P4 and P5. The distance progressively increases from the tunnel axis, therefore the two verticals at 10.0 m and 20.0 m are represented. In Fig. 5, all ratios are calculated with respect to point Q, located on the right-hand wall at one third of the wall height from the rail level (Fig. 2). Therefore, a description of the amplification or de-amplification of the magnitude of the computed acceleration with respect to the one at the tunnel is provided. As the system is linear, there are no differences for the two load combinations depicted in Fig. 3, even though for the sake of completeness, they are reported in Fig. 5, however. For both acceleration components, the role

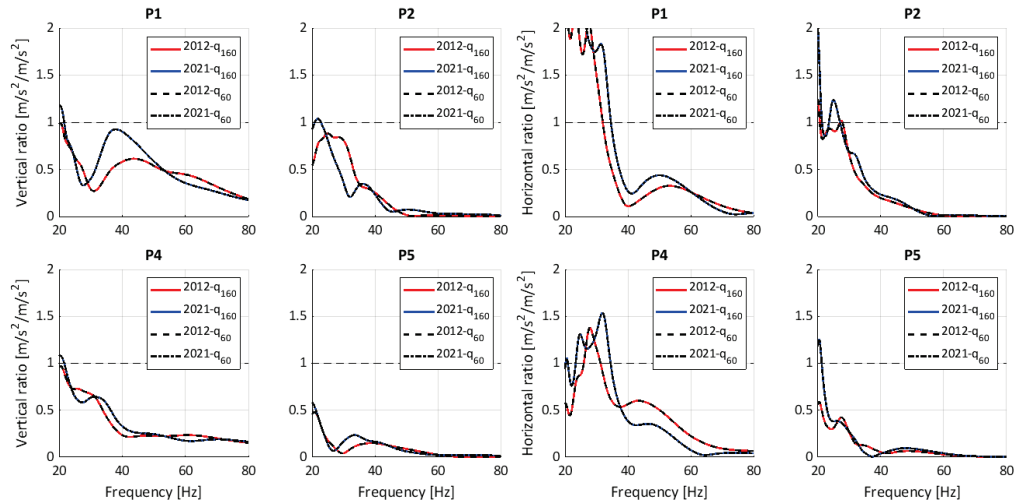


Figure 5 Acceleration spectral ratio for control points P1, P2, P4 and P5 on the ground and at a depth of 3.0 m (see Fig. 1). The ratios are calculated with respect to point Q at the right wall of the tunnel.

played by the different dynamic response of the soil is clear. Although the vertical ones undergo a de-amplification from the tunnel wall to the soil, their frequency content may change, as it may be shown by the peak at almost 40 Hz for the 2021 scenario which is not present in the 2012 one for P1, or the plateau exhibited by the second one for frequencies around 30 Hz and not registered by the first in P2. Amplifications can be highlighted for horizontal accelerations everywhere. Particular attention can be devoted to P1, where the signal doubles in the frequency range below 35 Hz, with a slightly more severe situation

depicted by the 2021 scenario. The increase of the horizontal acceleration at the ground for distances smaller than 5.0 m from the right wall naturally follows from the combination of the motions induced by the horizontal oscillations of the right diaphragm and the vibrations of the top slab. A conclusion which is consistent with the behaviour shown in Fig. 4. The comparison between P1 - P4 and P2 - P5 for both acceleration components highlights the passing from a volume-driven propagation mechanism to a surface one in which the role played by the tunnel movement is emphasized. The quality of the numerical

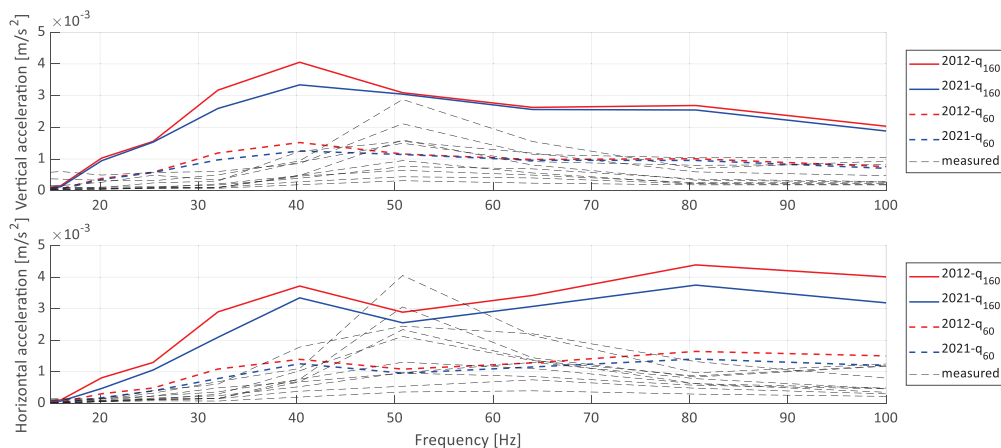


Figure 6 Comparison between Fourier amplitude spectra of measured acceleration at point Q in Fig. 2 and numerical predictions at varying soil dynamic response and static axle load of the train.

predictions is assessed comparing computed accelerations at the tunnel wall, i.e., point Q at the right diaphragm depicted in Fig. 2, with measures available for a similar M1 tunnel conducted by Metropolitana Milanese. The recordings provide one hour of train passages registrations. Among them, just 10 were selected for the comparison. Since the monitored tunnel is double track, at times the accelerometer recorded the simultaneous passage of two trains running in opposite directions. This explains the presence of spectra of the measured signal characterized by higher amplitudes than others (Fig. 6). The match between the measured and predicted acceleration is deemed to be satisfactory, despite the assumption of plain strain and the difference in the tracks unevenness and rail-track systems in the two configurations. The effect of the different static axle load can be clearly appreciated in the fact that the predicted spectra are pushed upwards assuming values comparable to the recorded double passages. Nonetheless, the matching between the recordings and the Q_{s60} simulation outlines the agreement between the effect induced by the passage of Leonardo trains along the M1 line and the used approach. Furthermore, a slightly different response of the tunnel is appreciated when the dynamic response of the soil changes over time. Higher horizontal accelerations are predicted with the 2012 model. This is deemed to be a consequence of the smaller Poisson coefficient and weight of the soil which surrounds the tunnel in this drier configuration. Recorded accelerations show a peak of variable magnitude at nearly 50 Hz. Even though its origin is not totally clear, the resonance frequency of the coupled wheel-track system may play a role. Nonetheless, this would explain the different behaviour of the simulated signals, as in the numerical models tracks were not reproduced. Hence, the shape of the calculated spectra is expected to be primarily related to the spectrum of the enforced load (Fig. 3).

4. CONCLUSIONS

A preliminary assessment on the role played by a change with time of the soil dynamic response as a consequence of different hydrological states in the propagation of ground borne vibrations from underground trains is provided. Two finite element numerical models are presented, recalling the different results from two geophysical tests campaigns carried out at the same site in Milano in March 2012 and April 2021. Furthermore, the role played by a change in the static weight of the train is taken into account and discussed. Although the predicted levels of weighted acceleration are similar in the two cases, namely 2012 and 2021, the variation in the dynamic response of the system,

resulting from a change in the measured and simulated impedance ratios, has been highlighted. This condition may be emphasized if the saturation and suction degree profiles become more markedly different.

5. REFERENCES

- [1] S. Gupta, Y. Stanus, G. Lombaert: "Influence of tunnel and soil parameters on vibrations from underground railways", *Journal of Sound and Vibration*, vol. 327, no. 1-2, pp. 70-91, 2009.
- [2] M. Schevenels, G. Degrandec, G. Lombaert: "The influence of the depth of the ground water table on free field road traffic-induced vibrations", *International journal for numerical and analytical methods in geomechanics*, vol. 28, no. 5, pp. 395-419, 2004.
- [3] D. P. Connolly, G. Kouroussis, O. Laghrouche, C.L. Ho, M.C. Forde: "Benchmarking railway vibrations—Track, vehicle, ground and building effects", *Construction and Building Materials*, vol. 92, pp. 64-81, 2015.
- [4] X. Qian, D. H. Gray, R.D. Woods: "Voids and granulometry: effects on shear modulus of unsaturated sands", *Journal of Geotechnical Engineering*, vol. 119, no. 2, pp. 295-314, 1993.
- [5] UNI11389 (in Italian), Ente nazionale italiano di normazione, Milano, IT, 2011.
- [6] Q-Y. Xu, X. Ou, F. Au, P. Lou, Z-C. Xiao: "Effects of track irregularities on environmental vibration caused by underground railway", *European Journal of Mechanics-A/Solids*, no. 59, pp. 280-93, 2016.
- [7] UN9614 (in Italian), Ente nazionale italiano di normazione, Milano, IT, 2011.
- [8] E. Vanmarcke, D. Gasparini: "Simulated earthquake ground motions", in *SMiRT 4* (San Francisco, USA), 1977.
- [9] N. Pontani, L. Martinelli, M. Acquati, C. Jommi: "A numerical assessment of variable saturation of the upper layers on the ground borne vibrations from underground trains: A case history", *Transportation Geotechnics*, no. 40, 2023.
- [10] MJ. Griffin, J. Erdreich: *Handbook of human vibration*. Academic Press, 1990.